Anisotropic and Isotropic Chemical Shifts Perturbations from Solid State NMR Spectroscopy for Structural and Functional Biology

24

Eduard A. Chekmenev, Joana Paulino, Riqiang Fu, and Timothy A. Cross

Contents

Introduction 506
Discussion: *Gramicidin A: Anisotropic Chemical Shift Perturbations* 509
Discussion: *M2 Proton Channel: Isotropic and Anisotropic Chemical Shift Perturbations* 513
Conclusions 516
References 517

Abstract

A molecular structure determined by crystallography, cryo-EM, or NMR is an excellent starting point for our understanding of how biology is accomplished, but NMR is one of the best tools for going beyond this starting point for a detailed characterization of functional mechanisms, even for an understanding of kinetic

E. A. Chekmenev (✉)
Institute of Imaging Science, Vanderbilt University, Nashville, TN, USA
e-mail: eduard.chekmenev@vanderbilt.edu

J. Paulino
Institute of Molecular Biophysics, Florida State University, Tallahassee, FL, USA

National High Magnetic Field Laboratory, Tallahassee, FL, USA
e-mail: joana.paulino@gmail.com

R. Fu
National High Magnetic Field Laboratory, Tallahassee, FL, USA
e-mail: rfu@magnet.fsu.edu

T. A. Cross
Institute of Molecular Biophysics, Florida State University, Tallahassee, FL, USA

National High Magnetic Field Laboratory, Tallahassee, FL, USA

Department of Chemistry and Biochemistry, Florida State University, Tallahassee, FL, USA
e-mail: cross@magnet.fsu.edu

G. A. Webb (ed.), *Modern Magnetic Resonance*,
https://doi.org/10.1007/978-3-319-28388-3_87

rates. To this end one of the best approaches for doing this is through the observation of isotropic and anisotropic chemical shift perturbations. Two molecular systems that have been extensively studied and characterized exemplify the usefulness of chemical shift perturbation as an effective strategy for understanding functional activities. **Gramicidin A**, an antibiotic from *Bacillus brevis*, that as a dimer forms a monovalent cation channel and a protein from *Influenza A virus*, the M2 protein that as a tetramer forms a proton channel. Blocking the **M2 proton channel** is an effective anti-influenza strategy. For gramicidin it was discovered that different monovalent cations have different binding sites at the mouth and exit of the channel accounting for the different solvation energy requirements of the various cations. For M2 the functional activity of a unique histidine tetrad that shuttles protons into the viral interior through a balance of futile and conductance protonation cycles was elucidated by chemical shift perturbations.

Keywords
Gramicidin A · M2 proton channel · Solid-state NMR · ^{15}N NMR · ^{17}O NMR · Anisotropic chemical shift interactions · Magic angle spinning ssNMR · Cation binding site · Oriented sample ssNMR · Isotropic chemical shift perturbations · Proton conductance

Introduction

NMR spectroscopy is one of the most versatile tools for the characterization of macromolecular structure and dynamics. While X-ray diffraction and crystallography have played a dominant role in the number of structural depositions to the Protein Data Bank (PDB), there have been limitations as to the proteins and protein domains that could be crystallized. Cryo-electron microscopy has made great strides recently, but here too there have been limitations associated with sample preparation and with dynamic domains. Indeed, this toolbox of NMR spectroscopy, X-ray crystallography, and cryo-EM is highly complementary. NMR has the unique advantages of being able to characterize proteins with dynamic domains and in native-like environments – a very important feature since protein structure is the result of the sum of molecular interactions within the protein and between the protein and its environment [1]. In addition, NMR is uniquely able to characterize molecular motions over a broad range of frequencies at atomic resolution. Since protein functional activities require dynamics, NMR is uniquely positioned to provide critical insights into functional mechanisms and even into explanations for kinetic rates.

The majority of proteins for which crystallization has been attempted do not yield high-resolution crystals; often regions or domains of proteins have to be excised for crystallization to be successful. This has recently come to the fore with the discovery of intrinsically disordered proteins (IDPs) and domains (IDDs) that have extensive dynamics. In fact, the broad scientific community has been very surprised by this discovery, because these crystal structures in the PDB provide no suggestion that highly dynamic domains exist in a majority of proteins. This is the result of selection

for those proteins and protein domains that form relatively rigid structures. In many cases the dynamic domains were removed to aid crystallization. Now, it is becoming apparent that these IDPs and IDDs are particularly important as regulatory regions of proteins, where multiple sites maybe phosphorylated resulting in what is now known as proteoforms. Mass spectrometry is playing an increasing role in the characterization of proteoforms [2]. The picture for many proteins that is now emerging is one in which these have a well-structured core with an additional domain or domains that are highly dynamic and functionally important. Maybe most importantly, as we look to the future of structural biology, is the characterization of nascent structure and the characterization of dynamics that have critical roles in functional and regulatory mechanisms. Once again, the combination of technologies for understanding the complexities of structural and functional biology is emphasized by the range of challenges that biology has provided for us to decipher.

In addition, many proteins exist in heterogeneous environments, such as lipid bilayers, or crowded environments that influence the structure and dynamics of proteins [3]. Indeed, it has been recognized since the early days by Christian Anfinsen that protein structure was the result of molecular interactions within the protein and between the protein and its environment [1]. Consequently, for membrane proteins the **solid-state NMR** ability to characterize proteins in a native like liquid crystalline lipid bilayer environment is critically important [3]. Poor models of this complex environment have led to many distorted and misleading protein structures. For crystallization of membrane proteins, often thermal stabilizing mutations are made before the structure can be crystallized in a detergent environment. Such mutations at a minimum suggest modifications to the protein dynamics, which of course is helpful for crystallization and diffraction, but can be misleading for the interpretation of the protein's functional mechanism. In addition, such mutations have been shown to lead to structural perturbations of the protein [4]. Such structural perturbations are typically only observed once the structure has been characterized in the absence of such mutations, which is often not possible.

Here, the NMR focus is on isotropic and **anisotropic chemical shift perturbations** as a tool for structural and functional biology. Isotropic chemical shifts result from the complete orientational averaging of chemical shift tensors. This happens in solution NMR experiments where the molecules, even large macromolecular structures, tumble rapidly on the time scale of the anisotropic interaction to average the spin interactions. This also happens in **magic-angle spinning** (MAS) solid-state NMR experiments where the samples that do not tumble rapidly in solution are spun fast compared to the anisotropic spin interactions at an angle of 54.7° with respect to the magnet field axis of the NMR spectrometer resulting in isotropic chemical shifts. In the absence of rapid tumbling of the protein either in solution or by MAS, anisotropic chemical shifts can be observed either representing a rigid protein site or one with partial averaging of the anisotropy, such as that from global rotation about a single axis or from limited amplitude motion of a peptide plane. In addition to chemical shifts, a number of other interactions, such as dipolar and quadrupolar interactions, can be averaged by molecular motions and evaluated. As an example, membrane proteins in liquid crystalline lipid bilayers will rotate about the bilayer

normal and wobble about this axis as well. The anisotropic spin interactions are particularly sensitive to the orientation of the nuclear site with respect to the magnetic field and to any motional axis that is present. As a result they are very sensitive to structural and dynamic perturbations that may occur during functional perturbations, such as ligand or ion binding.

Here, these NMR tools using two molecular systems illustrate the power of this methodology to characterize functional activities in two membrane bound systems. One of these is gramicidin A, an unusual 15 amino acid peptide with alternating L and D amino acids that forms a β-strand wrapped into a right-handed helix. All of the gramicidin sidechains are on the external surface facing the lipid environment. The polypeptide backbone has i to i + 7 hydrogen bonding resulting in 6.5 residues per turn based on **oriented sample** solid-state NMR (OS ssNMR) data (Fig. 1) [5, 6]. As an amino terminus to amino terminus dimer with both amino termini blocked with a formyl group, the structure forms a monovalent cation selective channel across membranes. The channel is stabilized in lipid bilayers by the interactions of four tryptophan residues in the C-terminal half of each monomer that hydrogen bond through their indole groups with the bilayer interfacial region [7]. The native structure of gramicidin had been hotly debated in the literature [8, 9]. In many crystallographic studies, a variety of intertwined double helical structures have been characterized (left-handed, right-handed, parallel, and antiparallel structures). However the native structure as described above was first reported by solution NMR in SDS micelles [10] and confirmed in a high-resolution structure in liquid crystalline DMPC lipid bilayers [5, 6]. While this debate was resolved in the mid-1990s with our high-resolution structure, additional crystallographic structures have appeared. In 1998 a double helical structure crystallized from glacial acetic acid was touted as the native structure without any demonstration that water could penetrate into and through the pore, never-mind cations [11]. In 2010 yet another left-handed double helical structure was obtained, this time from a lipidic cubic phase environment claiming to validate lipidic cubic phase crystallization as a proven approach for native-like small membrane protein structure crystallization [12]. Unfortunately, the pore, as before, did not sustain a single file of water molecules and was therefore not the native structure. However, the lipidic cubic phase is better than acetic acid that had been used as an earlier crystallization environment, but lipidic cubic phase is not a liquid crystalline lipid bilayer that uniquely supports the native structure of gramicidin.

The second molecular system that will be discussed in this manuscript is the M2 protein from *Influenza A virus* (Fig. 2). This is an essential protein for the virus that as a tetramer forms a proton channel or more accurately a transporter as protons covalently bind to histidyl residues from waters of the external aqueous environment and are then transferred to waters of the internal environment by sidechain structural rearrangements [13]. The His-37 residues are near the center of the transmembrane helix of the protein facing into the pore. The first structure of this protein was published in a pair of manuscripts in 2001 and 2002 of just the transmembrane helix (residues 22–46) based on OS ssNMR and a single interhelical distance in a liquid crystalline DMPC environment [14, 15]. In 2008 a structure of the M2 transmembrane helix (residues 19–46) crystallized in octylglucoside and xylitol

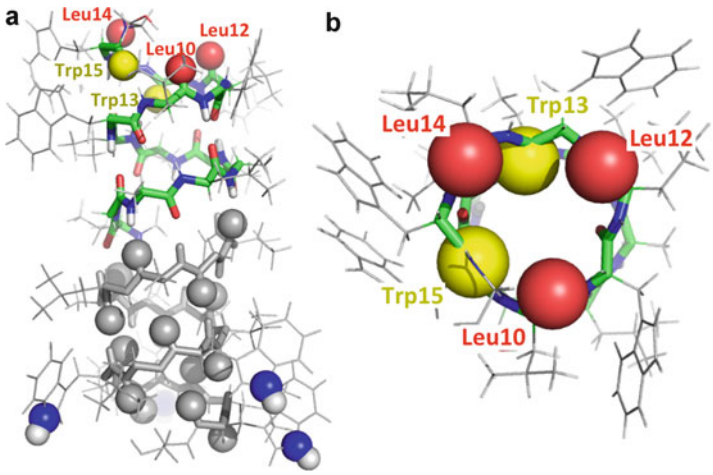

Fig. 1 Gramicidin structure (1MAG) highlighting the carbonyl oxygens (*space filling*) important for cation binding (*red*) and others in the binding sequence that do not appear to be involved in the binding site (*yellow*). (**a**) The dimeric structure of gramicidin A that spans the lipid bilayer. Only the Trp indole NH sites are highlighted (*blue*) in the lower monomer for clarity. These sites are important for stabilizing the channel orientation in the membrane. (**b**) View of the channel down the pore with the carbonyl oxygens highlighted as in (**a**)

was characterized as an asymmetric tetramer due to penetration of a detergent molecule between the transmembrane helices that hydrogen bonded with one of the functionally critical histidine residues disrupting the histidine tetrad and its symmetry [16]. In addition, a salt bridge formed between terminally charge residues of adjacent tetramers in the crystal lattice changing the tilt of the helices. A much better crystal structure of a slightly shorter construct (residues 25–46) also in octylglucoside was published in 2010 [17]. In the same year, a high-resolution structure of the conductance domain (22–62) was published that in addition to the transmembrane helix included the juxtamembrane amphipathic helix (Fig. 2) [18]. The more recent crystal structure and the OS ssNMR structure have considerable similarity except for the critical histidine tetrad. In the meantime, a solution NMR structure was published in 2008 of the conductance domain (residues 18–60) in a solution of DHPC detergent [19]. The helices had a much smaller tilt angle with respect to the pore axis resulting in a narrower pore that did not permit binding of the antiviral drug, rimantadine, in the pore. Instead, it bound to each helix external to the pore misleading the community about how this drug inhibits the protein.

Discussion: *Gramicidin A: Anisotropic Chemical Shift Perturbations*

The backbone structure was characterized using OS ssNMR of singly ^{15}N-labeled and singly ^{13}C carbonyl-labeled proteins designed to specifically label peptide bonds (^{15}N—^{13}C) in the polypeptide incorporated into DMPC lipid bilayers (Fig. 1).

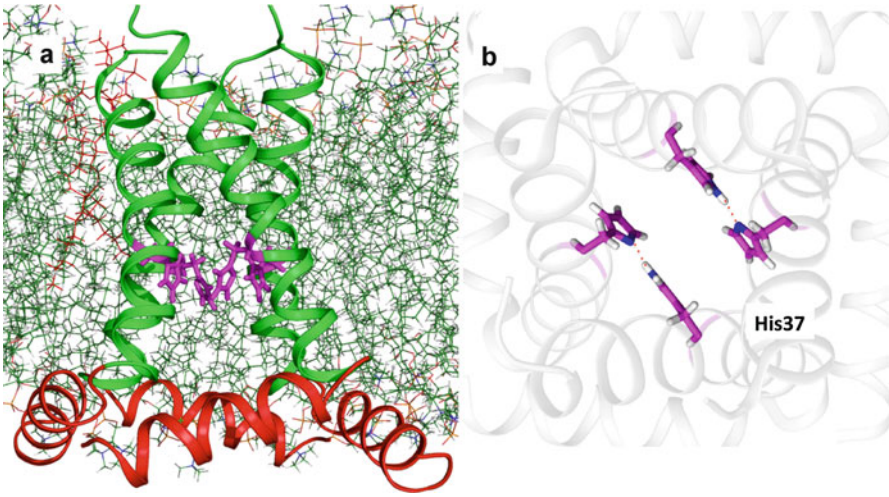

Fig. 2 M2 conductance domain in a liquid crystalline lipid bilayer environment. (**a**) Structure of the conductance domain in a DOPC/DOPE lipid bilayer characterized primarily from OS ssNMR restraints. The transmembrane helix is shown as a *green* ribbon, the juxtamembrane helix is shown as a *red* ribbon, and the sidechains of His37 tetrad are shown in *stick* form in *magenta*. (**b**) N-terminal view through the M2 proton pore highlights the interaction between the histidyl groups at pH 7.5. Hydrogen bonds between interacting His37 residues forming imidazole-imidazolium pairs are illustrated with *red dotted lines* which occur between Nε2H and Nδ1 sites. The nitrogen sites are *blue*

^{15}N anisotropic chemical shifts, ^{15}N—^{1}H, and ^{15}N—^{13}C dipolar interactions were obtained for almost every peptide plane yielding a precise orientation for each peptide plane with respect to the bilayer normal [20]. The backbone restraints resulted in an orientation for each peptide plane with an error bar of approximately ±2°. The dynamic axis and amplitude of many of the peptide planes were characterized both by the analysis of the averaging of ^{15}N anisotropy in unoriented samples compared to flash frozen samples and by field-dependent ^{15}N T_1 relaxation measurements [21, 22]. Each sidechain structure and dynamics were characterized by single sidechain labeling with ^{2}H and both unoriented powder pattern analysis and oriented sample analysis [23]. The four Trp residues were also characterized through ^{15}N indole powder pattern and oriented ^{15}N- and ^{2}H-labeled sample spectroscopy [7]. The result was a very high-resolution structure defining a structure with 6.5 residues per turn in a single-stranded helix. A complete cross-validation and R-factor calculation were performed documenting an RMS deviation of 0.11Å among the backbone atoms [24]. The sidechain structures had less precision, due to a greater motional amplitude, especially in Val_1 and Val_7 which undergo large amplitude three-state rotameric jumps, while Val_6 and Val_8 were shown to have a fixed rotameric state in liquid crystalline DMPC bilayers [23]. ^{2}H powder pattern analyses were also performed for the four Leu sidechains displaying relatively rigid structures as with Val_6 and Val_8. REDOR distances across the monomer-monomer junction proved that the structure was dimeric [25].

To go beyond structural biology to functional biology, anisotropic chemical shift perturbation was pursued. The polypeptide backbone that lines the pore wide enough only for a single file of water molecules was studied for **cation-binding** sites in the gramicidin channel [26]. For monovalent cations to pass through the pore, it must be stripped of all but two of its waters of solvation prior to entering the single file region of the pore. Presumably, these waters are replaced by carbonyl oxygens, and the first such oxygen that would be available at the mouth of the structure is the Leu_{14} carbonyl in the peptide plane with Trp_{15} Nα. The next nearest oxygen atom to the C-terminal end of the structure is the Leu_{12} carbonyl in the peptide plane with the Trp_{13} Nα and so on (Fig. 1). Recall that this is a β-strand type of structure with all of the sidechains on one side of the strand (due to alternating D and L residues) and consequently the peptide plane orientations alternate. In other words, the Trp_{15} and Trp_{13} carbonyls instead of being oriented toward the bulk aqueous environment are oriented toward the membrane interior. With single residue ^{15}N-labeled Trp residues (i.e., only one backbone site per sample), the perturbation of various cations on the orientation of the peptide planes could be evaluated using OS ssNMR. As shown in Fig. 3, different sites are influenced to a greater or lesser extent by the various cations. For Li^+ the Trp_{11} Nα (7.7.Å from the bilayer center) is influenced the most, implying that the carbonyl of Leu_{10} has the strongest interaction with Li^+. In binding each of the cations studied here to gramicidin A, the indole ^{15}Nε1 anisotropic chemical shift resonances of the Trp sidechains were not significantly influenced. This suggests that there is no significant change in the overall structure including the interaction of the indole sites with the bilayer interface. Moreover, observed changes in the ^{15}Nα—^{1}H dipolar couplings suggested changes of just 2–4° in the peptide plane orientations for these sites that demonstrate significant interaction with the cations. Yet the changes in chemical shift were very significant – up to 10 ppm. It was verified that the primary cause for the changes in chemical shift was due to induced polarization effects resulting in modifications of the tensor element magnitudes [27].

Based on the ^{15}Nα data with the divalent cation, Ba^{++}, in solution with the channel, only Leu_{12} and Leu_{14} carbonyls appear to have significant interactions with this ion (Fig. 3) [26]. Ba^{++} like other divalent cations does not transit through the gramicidin pore even though Ba^{++} has a very similar dehydrated radius as that of K^+, but it does bind at the opening of the channel pore with a much stronger binding constant than the monovalent cations [28]. For channels the goal is to provide enough solvation to strip the necessary waters from the cation to get the ion into and through the channel without forming a stable complex that blocks the channel. Ba^{++} appears to lack an interaction with the Leu_{10} carbonyl based on the lack of an interaction with the Trp_{11} ^{15}Nα resonance in the same peptide plane, but significantly influences the Trp_{13} and Trp_{15} ^{15}Nα sites. Both K^+ and Li^+ are conducted by the channel, and both influence all three Trp ^{15}Nα sites discussed here, although not in the same proportion. For Li^+ the energy required to strip off the waters in gas-phased hydrated cations, especially third and fourth waters of the 6 in the primary hydration shell is greater than that for K^+ [29]. Potentially, this explains the apparent stronger interaction with the Leu_{10} carbonyl compared to Leu_{12} for Li^+, while K^+ appears to have a stronger interaction with the Leu_{12} carbonyl instead of the Leu_{10} carbonyl. The overall stronger perturbation of the

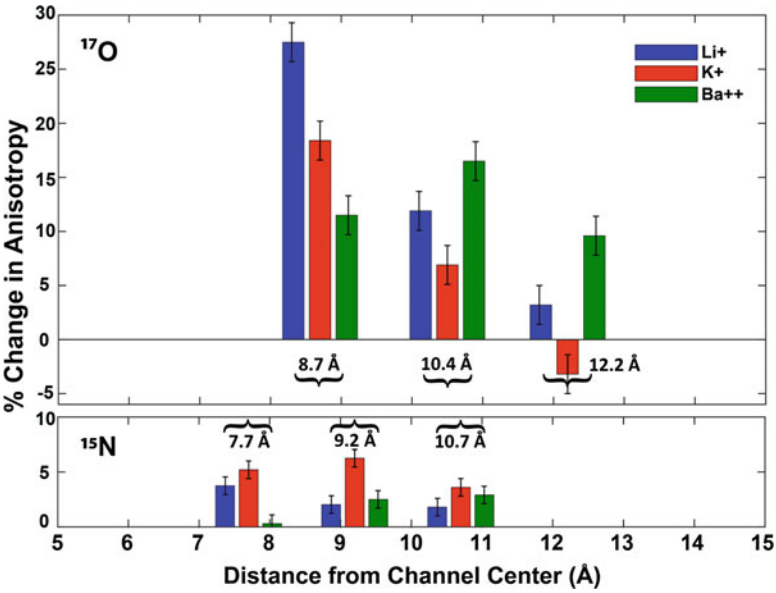

Fig. 3 Characterizing the cation-binding sites in gramicidin A. Anisotropic chemical shift perturbations of ^{15}N amide sites and ^{17}O carbonyl oxygen sites in the backbone structure. The three ^{17}O carbonyl oxygens exposed at the C-terminus of gramicidin to the aqueous environment belong to Leu_{14}, Leu_{12}, and Leu_{10} (Fig. 1). The corresponding amide Nα sites of the same peptide planes come from Trp_{15}, Trp_{13}, and Trp_{11}. These ^{15}N and ^{17}O resonances report on a change in orientation of the peptide plane or change in magnitudes of the tensor elements in response to cation binding. Here, the change in anisotropic chemical shift for binding Li^+ (*blue*), K^+ (*red*), and Ba^{++} (*green*) to the channel is reported as a fraction of the chemical shift anisotropy of the unbound state. The distance for the specific nitrogen and oxygen atoms from the channel center is identified. The ^{15}N data was previously published [26]

^{15}N resonances induced by K^+ compared with Li^+ may be explained by the stronger binding constant for K^+ [28]. The difference in the proportion of the perturbations suggests a somewhat different binding site for Li^+ and K^+ [26].

Studies of these interactions through ^{15}N-labeled backbone amides is an indirect approach. It would be far better to observe the carbonyl oxygen atoms directly, but ^{17}O in biological sites has a very large quadrupolar coupling constant ranging from 5 to 9 MHz. Consequently, both MAS and OS ssNMR linewidths are broad at currently available field strengths. However, single site ^{17}O-labeled gramicidin A has been aligned, as with ^{15}N-labeled samples described above, and observed for the three Leu sites that form the binding site for monovalent cations [30, 31]. Because these ^{17}O resonances have T_1 values in the submillisecond regime, and there is no need for proton decoupling, it is possible to take great advantage of rapid recycling of the experiment permitted by the short T_1. Consequently, an 8 ms recycle delay in a spin echo experiment was used to observe the ^{17}O spectra with high sensitivity [32, 33].

Even though the ^{17}O linewidths for the anisotropic carbonyl ^{17}O chemical shifts were on the order of 40 ppm, the chemical shift changes upon cation addition were

readily measured due to the high sensitivity of the experiments. Upon binding Li^+ to Leu_{10} ^{17}O-labeled gramicidin A, a 60 ppm shift was observed, binding of K^+ resulted in a 40 ppm shift, and only a 25 ppm shift was observed upon binding to Ba^{++} (Fig. 3). This shows a similar trend to that of the ^{15}N results described above, but interestingly Ba^{++} appears to significantly influence the Leu_{10} carbonyl oxygen, which was not implied by the ^{15}N results. For Leu_{12}-labeled gramicidin, a 26 ppm shift was observed for Li^+ and a 15 ppm shift for K^+, while a 36 ppm shift was observed for Ba^{++}. For Leu_{14}-labeled gramicidin, Li^+ induced a 7 ppm shift and K^+ induced a shift 7 ppm shift of opposite sign, while Ba^{++} showed 21 ppm shift of similar sign to that of Li^+. Clearly ^{17}O is particularly sensitive to the interactions of these ions. What is clear is that the balance of perturbations induced by Ba^{++} is shifted toward the C-terminus of gramicidin compared to those induced by the monovalent cations. Moreover, the change in ^{15}N anisotropic chemical shift compared to the full width of the powder pattern was in the most dramatic case only 5%. Here Li^+ induces a change in the anisotropic chemical shift of 60 ppm when the width of the chemical shift powder pattern is only ~220 ppm, a 28% change in the anisotropy.

The sensitivity of ^{17}O to cation binding provides a high-resolution tool for assessing the interactions of the cation to these carbonyl sites, dramatically showing that the monovalent cations only interact weakly with the Leu_{14} carbonyl since they have penetrated far into the mouth of the pore much further than Ba^{++}. With the high sensitivity ^{17}O data, even Ba^{++} is shown to have a significant interaction with the Leu_{10} carbonyl, while the ^{15}N data did not suggest such an interaction. Importantly, both the ^{15}N and ^{17}O data suggest a clear cation-binding mechanism in which a fully hydrated cation is stepwise dehydrated as it interacts with more carbonyl oxygens in the channel pore. The removal of the penultimate water prior to passage through the pore (the third water) is clearly the barrier that generates a minimum in the potential energy profile for the monovalent cation passage through the pore. The concept that different monovalent cations have different binding sites in gramicidin A is uniquely demonstrated by these anisotropic chemical shift perturbation studies.

As an example of **isotropic chemical shift perturbations** in our studies of cation binding to gramicidin A, the $^{13}C_1$-labeled Val_1 gA in DMPC liposomes showed two isotropic chemical shift resonances under MAS conditions, corresponding to two different C═O bond orientations for the Val_1-Gly_2 peptide plane. The presence of K^+ cations influenced the isotropic resonance of the C═O bond that was oriented slightly toward the channel axis, but not the C═O that is tilted slightly away from the channel axis. The chemical exchange cross peak between these two resonances confirmed that the gA channels are internally gated [34].

Discussion: *M2 Proton Channel: Isotropic and Anisotropic Chemical Shift Perturbations*

The M2 proton channel is another example of a molecular structure in which crystallography, solution NMR, and solid-state NMR have each produced multiple molecular structures that show the challenges for characterizing the native protein

structure of a small helical membrane protein. Such small helical membrane proteins represent the majority of all transmembrane proteins in prokaryotic genomes, while in eukaryotes the fraction of large helical membrane proteins is greater. M2 is a tetrameric structure of a 97 residue polypeptide having a 25 residue N-terminus in the viral exterior, a 21 residue transmembrane helix, an approximately 16 residue amphipathic helix that interacts with the lipid bilayer interfacial region, and a 35 residue water-soluble C-terminus in the viral interior.

The first structures were obtained primarily from OS ssNMR data of just the transmembrane peptide known as the transmembrane domain [14, 15] and suggested a large helical tilt angle of 38° with respect to the bilayer normal. The large tilt angle was soon shown to reflect a distortion induced by the sample preparation protocol in which organic solvents were used to mix the lipids and peptides. Instead of a 38° helical tilt, the preparations that avoided mixing the lipids and peptide in organic solvents resulted in tilt angles of 32° in DMPC lipid bilayers [35]. In 2010 a structure of what is known as the conductance domain, since it has conductance properties that are very similar to the wild-type protein, was characterized in DOPC/DOPE liquid crystalline lipid bilayers (Fig. 2) [18]. In this work, the N-terminal region of the transmembrane helix had a tilt of 32°, and the C-terminal portion of the helix had a tilt of 20°. The OS ssNMR restraints from the polypeptide backbone determined the orientation of the peptide plane relative to the fourfold symmetry axis and the bilayer normal that was aligned parallel with the magnetic field. The fourfold symmetry in the backbone is clear, in that multiple resonances are not observed for the helices. In 2010, at the time when this structure was deposited, a published distance restraint from ESR was used as an interhelical restraint. Since then many interhelical restraints have been obtained that are consistent with the structure, but a re-refinement has not been performed as yet [36–38].

In 2008 the first published X-ray structure of the transmembrane domain [16] displayed serious distortions induced by the octylglucoside detergent and lattice contacts. In 2010 a second transmembrane domain structure was published [17] that lacked the obvious distortions of the first structure and had a kinked helix quite similar to the tetrameric structure of the conductance domain published a few weeks later (as described above) except that the structure of the His and Trp tetrads were different and the amphipathic helix was not present in the crystal structure. The His tetrad at the heart of the conductance mechanism in the ssNMR structure has adjacent His_{37} residue pairs hydrogen bonded forming a local dimer of dimer structure, whereas the crystal structure had a fourfold symmetric structure with all of the imidazole nitrogen hydrogen bonded to waters.

In 2008 the first structure of the conductance domain was achieved by solution NMR [19] in an aqueous solution of the detergent, DHPC. A helical protein in lipid bilayers is constrained by the hydrophobic thickness of the bilayer and consequently the tilt of transmembrane helices, but in a prolate ellipsoidal detergent micelle, that constraint is very weak. The hydrophobic thickness is an ellipsoidal variable that can be influenced by the protein, and consequently the tilt of the helices observed in DHPC micelles was much less (16°) than in the lipid bilayer or even in a crystal lattice. The reduced tilt led to a reduced pore diameter and prevention of the antiviral

drug, rimantadine, from binding in the pore. Consequently, the manuscript promoted an erroneous mechanism for drug binding and conductance inhibition.

In 2007 [35] it was shown using OS ssNMR that the M2 transmembrane domain in the presence of amantadine, a close relative of rimantadine, had a kinked helix in which the N-terminus had a tilt of 32° and the C-terminal portion a reduced tilt of 21° very similar to the helical tilts observed in liquid crystalline lipid bilayers of the conductance domain in the absence of drug. Recently, isotropic chemical shift perturbation via MAS ssNMR demonstrated [39] that the Ser_{31} residue in the pore was highly sensitive to the presence of rimantadine resulting in a conclusion that the drug was bound in the pore. This was confirmed by a REDOR distance measurement between rimantadine and the Gly_{34} residue, another residue lining the pore [39].

Since the observation that the His_{37} residues formed imidazole-imidazolium pairs and that this implied cooperative proton binding with two of the four pKas being similar [40], there has been considerable debate in the literature largely driven by the crystal structures. In 2012 exciting $^{1}H—^{15}N$ correlation MAS spectroscopy of the transmembrane peptide at −28 °C and pH 4.5 showed imidazole $^{1}H_N$ resonances extending to 15 and potentially to 16 ppm that were interpreted as imidazolium-water hydrogen bonds, since these frequencies were also coupled to the water resonance at 4.8 ppm [41]. In addition, at 23 °C and pH 8.5, the ^{1}H resonances for water at ~5 ppm are correlated with ^{15}N resonances extending to the unusual protonated nitrogen frequency of 190 ppm or higher suggesting that it would be better to characterize these resonances in the full-length protein. Indeed, a study with the full-length protein [13] clearly demonstrated that the proton resonances extend to greater than 19 ppm in a pH 6.2 sample clearly demonstrating strong or low-barrier hydrogen bonds (Fig. 4a), a very clear demonstration of isotropic chemical shift perturbation leading to critical functional insights. In addition, it is clear that these imidazole-imidazolium hydrogen-bonded pairs are attacked by hydronium ions generating imidazolium sites hydrogen bonded with water (12 ppm) and that protons from water (~ pH 5) exchange with the imidazolium protons leading to resonance cross peaks with the unusual frequencies of 190 and 5 ppm in these HN spectra.

Moreover, the heterogeneity in the ^{1}H and ^{15}N chemical shifts displayed in Fig. 4a further suggested that the exact geometry of the imidazole-imidazolium hydrogen-bonded states vary considerably in these full-length M2 protein spectra in a liquid crystalline lipid bilayer environment, albeit at relatively low temperature. To explain this observation of a complex set of relatively stable structures, it has been proposed that there is heterogeneity in the tetrameric helical bundle (Fig. 2). Unlike many helical bundles that have glycine residues to facilitate stable packing of adjacent helices, M2 has no such glycine residues facilitating close and consequently stable packing; instead, there are multiple bulky sidechains in the helix-helix interfaces that appear to have different sidechain rotameric states leading to differences in the imidazole-imidazolium hydrogen-bonded distance of one or two tenths of an Angstrom.

Proton transport by M2 has now been shown to occur through the +3 charged state of the His_{37} tetrad. The state described in Fig. 2 has two pairs of imidazole-imidazolium hydrogen bonds, hence a +2 state. In the acidified endosome that has

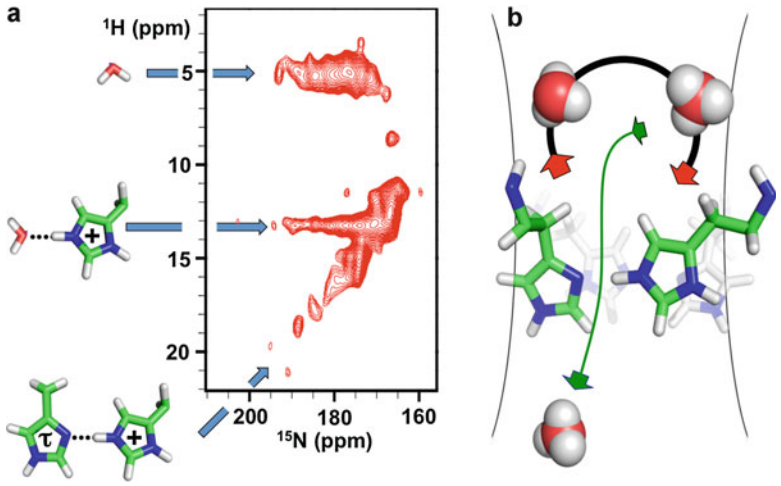

Fig. 4 Characterizing the imidazole-imidazolium hydrogen-bonded states in the M2 proton channel as a result of isotropic chemical shift perturbation. (**a**) NH correlation spectrum of ^{15}N imidazole-labeled His_{37} of M2 full-length protein. Three sets of resonances are identified: resonances from the imidazole-imidazolium hydrogen-bonded state at variable ^{1}H frequencies depending on the hydrogen bond length, resonances from the imidazolium hydrogen bonded with water at 13 ppm, and resonances from water following proton exchange with the imidazolium. (**b**) The conductance mechanism involves a futile and conductance cycles of protonation of the histidyl rings. In both cycles, protonation occurs from a hydronium ion in the pore exposed to the external environment of the virus. In the futile cycle, a proton from one of the imidazoliums is absorbed by a water in external pore. In the conductance cycle, a proton from one of the imidazoliums is absorbed by a water in the internal pore leading to acidification of the viral interior

encapsulated the viral particle, a hydronium ion protonates one of the two imidazoles of M2 forming a +3 state (Fig. 4b). This charge state is not stable and will revert to the +2 state when a water molecule captures one of these protons. If that water molecule is from the external environment, a futile cycle of protonation and deprotonation has taken place. If, however, the water is from the viral interior, transport of a proton from the viral exterior will have taken place leading to conductance of a proton across the viral membrane. Recently, a specific characterization of this exchange rate constant has been measured at -10°C and pH 6.2 of 1750 s^{-1} [42] further illustrating the qualitative and quantitative information that can be obtained from ssNMR.

Conclusions

The unique functional insights into cation binding and desolvation in the gramicidin pore and proton translocation through the M2 proton channel could only have been achieved with the tools afforded by NMR in the form of isotropic and anisotropic spin interaction perturbations. Oriented Sample ssNMR can be used to provide

numerous anisotropic structural restraints that have a high degree of precision. The interpretation of the perturbations to these interactions induced by ion or drug binding can be complex in that it could be a structural perturbation that is interpreted as a change in the orientation of the spin interaction with respect to the magnetic field or it may be a perturbation that changes the magnitudes of the spin interaction tensor elements. In either case, relative magnitudes, i.e., perturbations, can be evaluated as the relative strength of interactions between ligand and protein leading to unique insights into the functional biology of the molecular system. Of course, this approach is not restricted to anisotropic spin interaction perturbations, as seen with the perturbations induced by pH in the His_{37} tetrad of the M2 protein. The heterogeneity of the histidine resonances led not only to a unique description of the M2 proton channel functional mechanism but to a unique hypothesis for the origination of the heterogeneity in helix packing of this tetrameric protein. Indeed, this may be the first time that heterogeneity in tetramer packing of proteins has been observed. Consequently, both anisotropic and isotropic perturbations have led to important functional characteristics for these two biological systems. The initial ^{17}O results are particularly exciting as they were shown here to be a remarkably sensitive tool for characterizing cation binding in a channel. The advent of high-temperature superconductors leading to the availability of much higher magnetic fields for ^{17}O NMR spectroscopy suggest that dramatic gains in sensitivity and resolution will be forthcoming in the near future leading to many more insights into functional biology.

References

1. Anfinsen CB. Principles that govern the folding of protein chains. Science. 1973;181 (96):223–30.
2. Anderson LC, DeHart CJ, Kaiser NK, Fellers RT, Smith DF, Greer JB, et al. Identification and characterization of human proteoforms by top-down LC-21 tesla FT-ICR mass spectrometry. J Proteome Res. 2016;16:1087–1096.
3. Zhou HX, Cross TA. Influences of membrane mimetic environments on membrane protein structures. Annu Rev Biophys. 2013;42:361–92.
4. Cross TA, Ekanayake V, Paulino J, Wright A. Solid state NMR: The essential technology for helical membrane protein structural characterization. J Magn Reson. 2014;239:100–9.
5. Ketchem RR, Hu W, Cross TA. High-resolution conformation of gramicidin A in a lipid bilayer by solid-state NMR. Science. 1993;261(5127):1457–60.
6. Ketchem RR, Roux B, Cross TA. High-resolution polypeptide structure in a lamellar phase lipid environment from solid-state NMR derived orientational constraints. Structure. 1997;5:1655–69.
7. Hu W, Lazo ND, Cross TA. Tryptophan dynamics and structural refinement in a lipid bilayer environment: solid state NMR of the gramicidin channel. Biochemistry. 1995;34 (43):14138–46.
8. Cross TA, Arseniev A, Cornell BA, Davis JH, Killian JA, Koeppe RE, et al. Gramicidin channel controversy – revisited. Nat Struct Biol. 1999;6(7):610–2.
9. Andersen OS, Apell H-J, Bamberg E, Busath DD, Koeppe REI, Sigworth FJ, et al. Gramicidin channel controversy – the structure in a lipid environment. Nat Struct Biol. 1999;6:609.
10. Arseniev AS, Barsukov IL, Bystrov VF, Lomize AL, Ovchinnikov YA. 1H-NMR study of gramicidin A transmembrane ion channel. Head-to-head right-handed, single-stranded helices. FEBS Lett. 1985;186(2):168–74.

11. Burkhart BM, Li N, Langs DA, Pangborn WA, Duax WL. The conducting form of gramicidin A is a right-handed double-stranded double helix. Proc Natl Acad Sci U S A. 1998;95 (22):12950–5.
12. Hofer N, Aragao D, Caffrey M. Crystallizing transmembrane peptides in lipidic mesophases. Biophys J. 2010;99(3):L23–5.
13. Miao Y, Fu R, Zhou HX, Cross TA. Dynamic short hydrogen bonds in histidine tetrad of full-length M2 proton channel reveal tetrameric structural heterogeneity and functional mechanism. Structure. 2015;23(12):2300–8.
14. Wang J, Kim S, Kovacs F, Cross TA. Structure of the transmembrane region of the M2 protein H (+) channel. Protein Sci. 2001;10(11):2241–50.
15. Nishimura K, Kim S, Zhang L, Cross TA. The closed state of a H+ channel helical bundle: combining precise orientational and distance restraints from solid state NMR. Biochemistry. 2002;41:13170–7.
16. Stouffer AL, Acharya R, Salom D, Levine AS, Di Costanzo L, Soto CS, et al. Structural basis for the function and inhibition of an influenza virus proton channel. Nature. 2008;451:596–9.
17. Acharya R, Carnevale V, Fiorin G, Levine BG, Polishchuk AL, Balannik V, et al. Structure and mechanism of proton transport through the transmembrane tetrameric M2 protein bundle of the influenza A virus. Proc Natl Acad Sci U S A. 2010;107(34):15075–80.
18. Sharma M, Yi M, Dong H, Qin H, Peterson E, Busath DD, et al. Insight into the mechanism of the influenza A proton channel from a structure in a lipid bilayer. Science. 2010;330 (6003):509–12.
19. Schnell JR, Chou JJ. Structure and mechanism of the M2 proton channel of influenza A virus. Nature. 2008;451:591–5.
20. Ketchem RR, Lee KC, Huo S, Cross TA. Macromolecular structural elucidation with solid-state NMR-derived orientational constraints. J Biomol NMR. 1996;8(1):1–14.
21. Lazo ND, Hu W, Lee KC, Cross TA. Rapidly-frozen polypeptide samples for characterization of high definition dynamics by solid-state NMR spectroscopy. Biochem Biophys Res Commun. 1993;197(2):904–9.
22. North CL, Cross TA. Correlations between function and dynamics: time scale coincidence for ion translocation and molecular dynamics in the gramicidin channel backbone. Biochemistry. 1995;34(17):5883–95.
23. Lee KC, Huo S, Cross TA. Lipid-peptide interface: valine conformation and dynamics in the gramicidin channel. Biochemistry. 1995;34(3):857–67.
24. Kim S, Quine JR, Cross TA. Complete cross-validation and R-factor calculation of a solid-state NMR derived structure. J Am Chem Soc. 2001;123(30):7292–8.
25. Fu R, Cotten M, Cross TA. Inter- and intramolecular distance measurements by solid-state MAS NMR: determination of gramicidin A channel dimer structure in hydrated phospholipid bilayers. J Biomol NMR. 2000;16(3):261–8.
26. Tian F, Cross TA. Cation transport: an example of structural based selectivity. J Mol Biol. 1999;285(5):1993–2003.
27. Tian F, Cross TA. Cation binding induced changes in 15N CSA in a membrane-bound polypeptide. J Magn Reson. 1998;135(2):535–40.
28. Hinton JF, Whaley WL, Shungu D, Koeppe 2nd RE, Millett FS. Equilibrium binding constants for the group I metal cations with gramicidin-A determined by competition studies and T1+-205 nuclear magnetic resonance spectroscopy. Biophys J. 1986;50(3):539–44.
29. Dzidic JaK P. Hydration of the alkali ions in the gas phase. Enthalpies and entropies of reactions $M^+(H_2O)_{n-1} + H_2O = M^+(H_2O)_n$. J Phys Chem. 1970;74:1466–74.
30. Hu J, Chekmenev EY, Gan Z, Gor'kov PL, Saha S, Brey WW, et al. Ion solvation by channel carbonyls characterized by 17O solid-state NMR at 21T. J Am Chem Soc. 2005;127 (34):11922–3.
31. Fu R, Brey WW, Shetty K, Gor'kov P, Saha S, Long JR, et al. Ultra-wide bore 900 MHz high-resolution NMR at the National High Magnetic Field Laboratory. J Magn Reson. 2005;177 (1):1–8.

32. Chekmenev EY, Waddell KW, Hu J, Gan Z, Wittebort RJ, Cross TA. Ion-binding study by 17O solid-state NMR spectroscopy in the model peptide Gly-Gly-Gly at 19.6T. J Am Chem Soc. 2006;128(30):9849–55.
33. Chekmenev EY, Gor'kov PL, Cross TA, Alaouie AM, Smirnov AI. Flow-through lipid nanotube arrays for structure-function studies of membrane proteins by solid-state NMR spectroscopy. Biophys J. 2006;91(8):3076–84.
34. Jones TL, Fu R, Nielson F, Cross TA, Busath DD. Gramicidin channels are internally gated. Biophys J. 2010;98(8):1486–93.
35. Li C, Qin H, Gao FP, Cross TA. Solid-state NMR characterization of conformational plasticity within the transmembrane domain of the influenza A M2 proton channel. Biochim Biophys Acta. 2007;1768(12):3162–70.
36. Miao Y, Qin H, Fu R, Sharma M, Can TV, Hung I, et al. M2 proton channel structural validation from full-length protein samples in synthetic bilayers and *E. coli* membranes. Angew Chem Int Ed Eng. 2012;51:8383–6.
37. Miao Y, Cross TA, Fu R. Identifying inter-residue resonances in crowded 2D C- C chemical shift correlation spectra of membrane proteins by solid-state MAS NMR difference spectroscopy. J Biomol NMR. 2013;56:265–73.
38. Ekanayake EV, Fu R, Cross TA. Structural influences: cholesterol, drug, and proton binding to full-length influenza A M2 protein. Biophys J. 2016;110(6):1391–9.
39. Wright AK, Batsomboon P, Dai J, Hung I, Zhou HX, Dudley GB, et al. Differential binding of rimantadine enantiomers to influenza A M2 proton channel. J Am Chem Soc. 2016;138 (5):1506–9.
40. Hu J, Fu R, Nishimura K, Zhang L, Zhou HX, Busath DD, et al. Histidines, heart of the hydrogen ion channel from influenza A virus: toward an understanding of conductance and proton selectivity. Proc Natl Acad Sci U S A. 2006;103(18):6865–70.
41. Hong M, Fritzsching KJ, Williams JK. Hydrogen-bonding partner of the proton-conducting histidine in the influenza M2 proton channel revealed from 1H chemical shifts. J Am Chem Soc. 2012;134(36):14753–5.
42. Fu R, Miao Y, Qin H, Cross TA. Probing hydronium ion histidine NH exchange rate constants in the M2 channel via indirect observation of dipolar-dephased 15N signals in magic-angle-spinning NMR. J Am Chem Soc. 2016;138(49):15801–4.